

FEDSM-ICNMM2010-30742

Large eddy simulation of turbulent air flow over a surface mounted hemisphere

M.M. Tavakol

School of Mechanical
Engineering
Shiraz, Iran
tavakolmm@shirazu.ac.ir

O. Abouali

School of Mechanical
Engineering
Shiraz, Iran
abouali@shirazu.ac.ir

M. Yaghoubi

School of Mechanical
Engineering
Shiraz, Iran
yaghoubi@shirazu.ac.ir

ABSTRACT

Turbulent air flow around a surface mounted hemisphere is investigated numerically. The flow field has been simulated using Large Eddy Simulation (LES) technique. Using LES results, variations of flow velocity at various sections along the midplane are presented and compared with the wind tunnel measurements. Also the results of LES are compared with a RANS model ($k-\epsilon$ RNG). It is concluded that LES with the proper grid resolution is capable to capture the complex features of the flow especially in the separation bubble formed behind the hemisphere. The LES results are in a better agreement with experimental data compared with $k-\epsilon$ RNG model. Also various SGS models for LES technique are tested and the predictions of these models are compared.

INTRODUCTION

Turbulent flow around surface mounted obstacles is important for different engineering applications. Flow around buildings, wings, bridge pier and electronic devices are some examples of this type of flow. The interference between separated shear flow and the approaching boundary layer flow causes the formation of complex vortical structures which are responsible for turbulent dispersion, high pressure fluctuations and high heat and mass transfer rates. Additional complexity arises for curved bluff bodies like cylinders and hemispheres due to Reynolds number dependency of separation and reattachment process in subcritical regimes. Domed or vaulted roofs with hemispherical and cylindrical shapes are examples for these types of bluff bodies which are used as common roofs in the hot-arid regions of Iran. There are numbers of experimental and numerical studies about turbulent flow field around domes or wall mounted hemispheres.

Maher [1] presented a wind tunnel study in a low turbulence thin boundary layer flow to obtain pressure

distribution on a dome roof. Savory and Toy [2,3] conducted wind tunnel measurement to find the velocity and pressure distribution around hemisphere and hemisphere-cylinders for different incoming velocity and turbulent intensities. Yaghoubi [4] performed flow visualization by smoke wire technique and reported air flow pattern for different dome roof configurations. It is concluded that buildings location, spacing, height and arrangement are important factors which are considerably affect the flow field. Tamura et al. [5] did three-dimensional unsteady numerical simulation to obtain flow around a hemisphere, as typical shape of a dome. They reported the separation point over the hemisphere located at $X/D=0.1$ from the dome apex and the reattachment point located at $X/D=1$ from the dome center for flow Reynolds number (based on diameter of hemisphere) equal to 20000. Meroney et al. [6] studied wind loads on smooth, rough and dual domes immersed in a thick boundary layer. They performed wind tunnel measurement and numerical simulation to determine wind loads on domes. They presented the pressure distribution at different regions in streamwise and spanwise directions. Their numerical results indicated that the turbulence model does not seem critical in the prediction of pressure distribution over the hemisphere located in the thick boundary layer. Recently, Tavakol et al. [7] performed experimental and numerical studies to find flow field around a surface mounted hemisphere for different boundary layer flows. The hot-film anemometry as well as numerical simulation using RNG $k-\epsilon$ turbulence model are performed and the velocity distribution, streamwise turbulent intensity at different locations are reported for two different boundary layer flows. More recently, Cheng and Liu [8] conducted wind tunnel studies to investigate the mean and fluctuation pressure distribution over the domes. The case of smooth flow and thick boundary layer profile are considered and the critical Reynolds

number (i.e. the Reynolds number in which pressure field becomes Reynolds number independent) is reported to be 300,000 for smooth flow and 100,000-200,000 for thick turbulent boundary layer profile.

In the previous study of present authors [7] the RNG k- ϵ turbulence model is employed for numerical simulation which is not capable to accurately predict the behavior of flow field especially in the recirculation zone behind the hemisphere. In the present study Large Eddy Simulation (LES) technique is employed for numerical simulation of flow around surface mounted hemisphere and the results are compared with the wind tunnel measurements. Different sub-grid scale models are applied and the results are compared with the wind tunnel measurements.

NOMENCLATURE

D	Hemisphere diameter
E	Turbulent dissipation rate
H	Kolmogorov length scale
k	Turbulent kinetic energy
L	Larger turbulent length scale
L_{ij}	Germano identity
p	Pressure
Re	Reynolds number
S_{ij}	Rate of strain
T	Larger eddy time scale
t	Physical time step
t^*	Non-dimensional time step
u_i	Mean velocity
X_r	Reattachment length
X	Streamwise direction
Y	Vertical direction
Z	Spanwise direction
τ	Kolmogorov time scale
λ_t	Taylor time scale
ν_t	Sub-grid scale viscosity
ν	Kinematic viscosity
g_{ij}	Velocity gradient tensor
τ_{ij}^{sgs}	Sub-grid scale stress
T_{ij}^{sgs}	Sub-test scale stress
Δ	Grid filter

COMPUTATIONAL DOMAIN AND BOUNDARY CONDITIONS

Figure 1 shows the configuration of the computational domain. A hemisphere with 12 cm diameter is placed on the tunnel surface and the dimensions of computational domain are selected equal to wind tunnel test section [7]. The origin of coordinate system is selected at the center of hemisphere. The computational domain is $13.2D \times 3.8D \times 3.8D$ in X, Y and Z directions respectively, where X is streamwise direction, Y is normal to the surface and Z is spanwise direction.

Plane ABCD is the inlet boundary and velocity profile obtained from hot-wire measurement in the wind tunnel is used for this plane [7]. Zero gradient condition in x direction is applied for plane EFGH. For planes AEHD, BFGC, ABFE, CGHD and on the surface of hemisphere no slip boundary condition is employed.

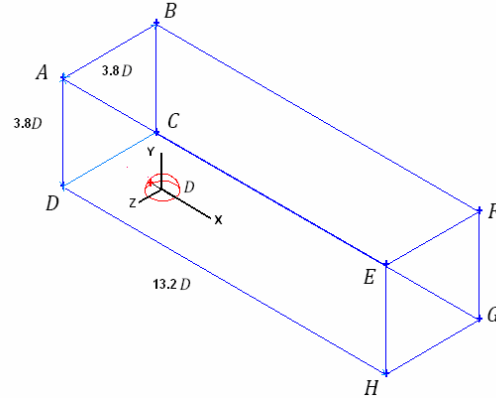


Fig. 1: Computational domain

The computational domain is discretized using a structured grid similar to the previous study of Tavakol et al. [7]. Figure 2 shows the grid arrangement in the computational domain. The finer grid is used near the hemisphere where the velocity gradients are large and the grid resolution is gradually decreased far from hemisphere where the flow is without any considerable variation. Total number of 1,100,000 computational cells is used for the initial sturdy of flow field and then the number of grid cells is increased to 4,200,000 cells to obtain a better prediction of flow field.

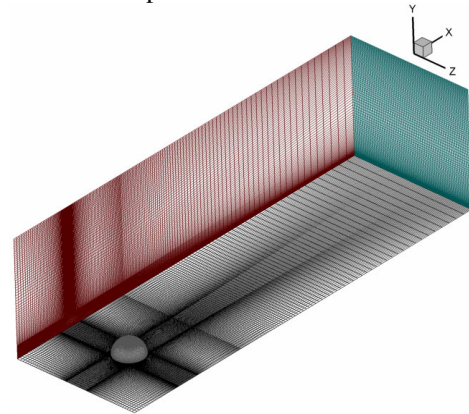


Fig. 2: Grid arrangement

NUMERICAL MODEL

Large eddy simulation (LES) technique is applied to simulate turbulent flow field around a surface-mounted hemisphere. In this theory it is assumed that large eddies of flow are dependent on the flow geometry, whereas the smaller

eddies are self-similar, therefore the large scale motions of the flow are calculated and the smaller universal scales are modeled using a sub-grid scale model. In practice, one is required to solve the filtered Navier-Stokes equations. The filtered continuity and Navier-Stokes equations for incompressible flow without body force can be written as:

$$\frac{\partial \bar{u}_i}{\partial x_i} = 0 \quad (1)$$

$$\frac{\partial \bar{u}_i}{\partial t} + \frac{\partial \bar{u}_i \bar{u}_j}{\partial x_j} = -\frac{1}{\rho} \frac{\partial \bar{p}}{\partial x_i} + \frac{\partial}{\partial x_j} \left(\nu \frac{\partial \bar{u}_i}{\partial x_j} \right) - \frac{\partial \tau_{ij}^{SGS}}{\partial x_j} \quad (2)$$

In this equations \bar{u}_i are the filtered velocity components, \bar{p} is the pressure, ρ is the fluid density and ν is the kinematic viscosity of fluid.

The last term on the right hand side of second equation is called sub-grid scale stress which is modeled based on the Boussinesque eddy viscosity approximation, i.e.:

$$\tau_{ij}^{SGS} - \frac{1}{3} \tau_{kk}^{SGS} \delta_{ij} = -2\nu_t \bar{S}_{ij} \quad (3)$$

In this equation δ_{ij} is Kronecker delta, \bar{S}_{ij} is the resolved-scale strain rate tensor and ν_t is the SGS eddy viscosity. The resolved-scale strain rate tensor is defined as:

$$\bar{S}_{ij} = \frac{1}{2} \left(\frac{\partial \bar{u}_i}{\partial x_j} + \frac{\partial \bar{u}_j}{\partial x_i} \right) \quad (4)$$

In the present study, the wall adopting eddy viscosity model (WALE model), dynamic Smagorinsky model and KETM (kinetic energy turbulence model) are used for computation of SGS eddy viscosity. In the WALE model SGS eddy viscosity is expressed as:

$$\nu_t = C_w \Delta^2 \frac{(S_{ij}^d S_{ij}^d)^{3/2}}{(\bar{S}_{ij} \bar{S}_{ij})^{5/2} + (S_{ij}^d S_{ij}^d)^{5/4}} \quad (5)$$

Where

$$S_{ij}^d = \frac{1}{2} \left(\bar{g}_{ij}^2 + \bar{g}_{ji}^2 \right) - \frac{1}{3} \bar{g}_{ij}^2 \bar{g}_{kk}^2 \quad (6)$$

$$\bar{g}_{ij} = \frac{\partial \bar{u}_i}{\partial x_j}$$

Here Δ is filter width which is specified from cube root of the cell volume and C_w is the coefficient of the model. The sub-grid scale stress tensor subjected to the test filter is given as:

$$T_{ij}^{SGS} = \hat{\hat{u}}_i \hat{\hat{u}}_j - \hat{\hat{u}}_i \hat{\hat{u}}_j \quad (7)$$

The resolved stress corresponding to the test filter applied to \bar{U} is the Leonard stress (L_{ij}). It is equal to difference between sub-grid and sub-test scale stress:

$$L_{ij} = T_{ij}^{SGS} - \tau_{ij}^{SGS} \sqrt{a^2 + b^2} \quad (8)$$

This equation is known as Germano identity. In this equation

T_{ij}^{SGS} and τ_{ij}^{SGS} have to be modeled while the Leonard stress L_{ij} can be obtained explicitly. Using the Smagorinsky model as the base model the Leonard stress can be evaluated from the resolved velocity field in LES and the Smagorinsky coefficient C_s which is a function of space and time can be estimated. This coefficient in dynamic Smagorinsky model is defined as

$$C_s = \frac{1}{2} \frac{L_{ij} S_{ij}}{M_{ij} \bar{S}_{ij}} \quad (9)$$

Where

$$M_{ij} = \Delta_{test}^2 \left| \bar{S}_{ij} \right| \left| \bar{S}_{ij} - \Delta^2 \bar{S}_{ij} \right| \bar{S}_{ij} \quad (10)$$

In KETM model, in order to obtain sub-grid scale viscosity one can solve additional filtered transport equation for the sub-grid scale

$$\frac{\partial \bar{\rho} k_{SGS}}{\partial t} + \frac{\partial \bar{\rho} k_{SGS} \bar{u}_j}{\partial x_j} = \frac{\partial}{\partial x_j} \left(\mu_{SGS} \frac{\partial k_{SGS}}{\partial x_j} \right) + \left(2\mu_{SGS} \bar{S}_{ij} - \frac{2}{3} \bar{\rho} k_{SGS} \delta_{ij} \right) - \bar{\rho} C_\epsilon \frac{k_{SGS}^{3/2}}{\Delta} \quad (11)$$

Solving this equation for k_{SGS} the sub-grid scale viscosity is obtained as $\nu_{SGS} = C_k \Delta k_{SGS}^{1/2}$.

The grid sizes in the computational domain and proper time step for unsteady simulation are two important parameters in every LES simulation. The size of grid cells in the computational domain is selected based on the previous study of present authors in the numerical simulation of same geometry using turbulence modeling. In order to obtain a proper time step size different time scales at several locations in the flow field are calculated using steady simulation via k- ϵ model. According to Baggett et al. [9] the grid filter should be

at least one-tenth of larger scales ($L = \frac{k^{3/2}}{\epsilon}$). In addition to the

larger scales and filter width other important time scales, i.e.

Taylor scales ($\lambda = \left(\frac{10\nu k}{\epsilon} \right)^{1/2}$) and Kolmogorov scales ($\eta = \left(\frac{\nu^3}{\epsilon} \right)^{1/4}$)

are also computed and compared with grid filter. The numerical simulations are performed using a non-dimensional

time step of $t^* = 0.0375$, ($t^* = \frac{tU}{D}$) for $Re_D = 30000$. This time

step is selected such that the time scale of resolved eddies is much less than the time scale of larger eddies ($T = \frac{k}{\epsilon}$) and

close to the time scale of smaller eddies (Taylor time scales, $\lambda_t = \left(\frac{15\nu}{\epsilon} \right)^{1/2}$). Numerical solution of the governing

equations is based on the finite volume method. The discretization of convective terms is performed using bounded central difference scheme developed by Leonard [10] and a fully second order implicit scheme is applied for temporal discretization. The SIMPLE algorithm is used to treat pressure velocity coupling in the flow field. Residuals of continuity and momentum equations at each time step are reduced to 10^{-5} . Numerical simulation is started using steady state solution via k- ϵ model. The converged solution obtained from k- ϵ model is used as the initial condition for large eddy simulation.

RESULTS

Numerical computations are performed using LES to obtain turbulent air flow field around a surface mounted hemisphere. Three different sub-grid scale eddy viscosities are applied in this study e.g, dynamic Smagorinski, WALE and KETM models. Numerical solutions are carried for $Re_D = 30000$ based on the free stream velocity and the hemisphere diameter. The solution procedure is started using steady state simulation via k- ϵ model following with unsteady LES simulation. The data sampling from unsteady solution is started after approximately 3000 time steps with $\Delta t = 0.0005$ s. At least 100 dimensionless time units (t^+) are taken with each sub-grid scale model to obtain reliable statistical data. The value of y^+ at the most cells of wall boundaries and the hemisphere surface is lower than 9.

The initial numerical simulation is performed using low resolution grid with total number of 1,100,000 grid cells and then the number of grid cells are increased to 4,200,000 to check the grid independency of numerical results. Figure 3 shows the comparison between numerical simulation using LES with different grid resolution, RNG k- ϵ model and the experimental data. It is clear that the predictions of RNG k- ϵ model and LES with low resolution grid are in poor agreement with the wind tunnel measurements. The LES simulation with high resolution grid shows very good agreement with the experimental data and the maximum reversed flow velocity and the height of shear layer are predicted with good accuracy. Figure 4 presents the similar comparison between the numerical results and the experimental data over the hemisphere at symmetry plane. Again, the prediction of LES with higher grid cells shows better agreement with respect to the experimental data. The previous study of authors shows that the RNG k- ϵ model can not predict the streamwise velocity near the hemisphere apex where the flow velocity is increased due to favorable pressure gradient over the hemisphere [7].

Based on the LES simulation with two grid resolution, the high resolution grid with approximately 4,200,000 computational cells is selected and the numerical simulation is done for different sub-grid scale eddy viscosity models. Results are presented for mean flow streamlines at various planes in the streamwise and spanwise directions. Also, velocity profiles

are plotted at various sections and compared with the experimental measurements.

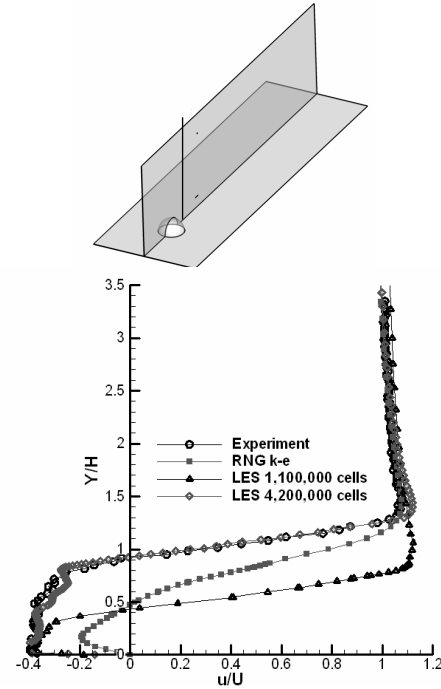


Fig. 3: Comparison between numerical results and experimental data at $X/D = 0.67$ on plane of symmetry

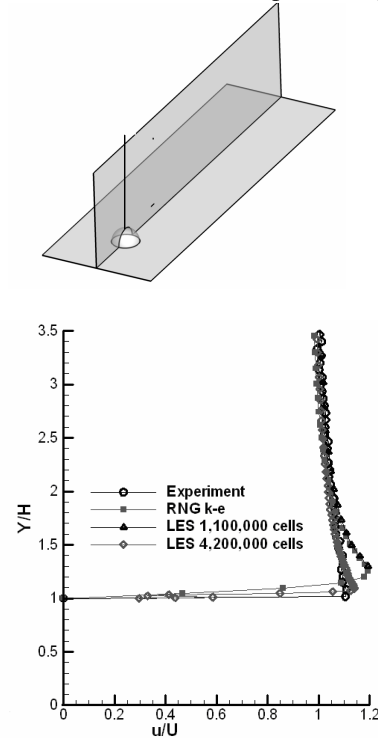


Fig. 4: Comparison between numerical results and experimental data at $X/D = 0$ on plane of symmetry

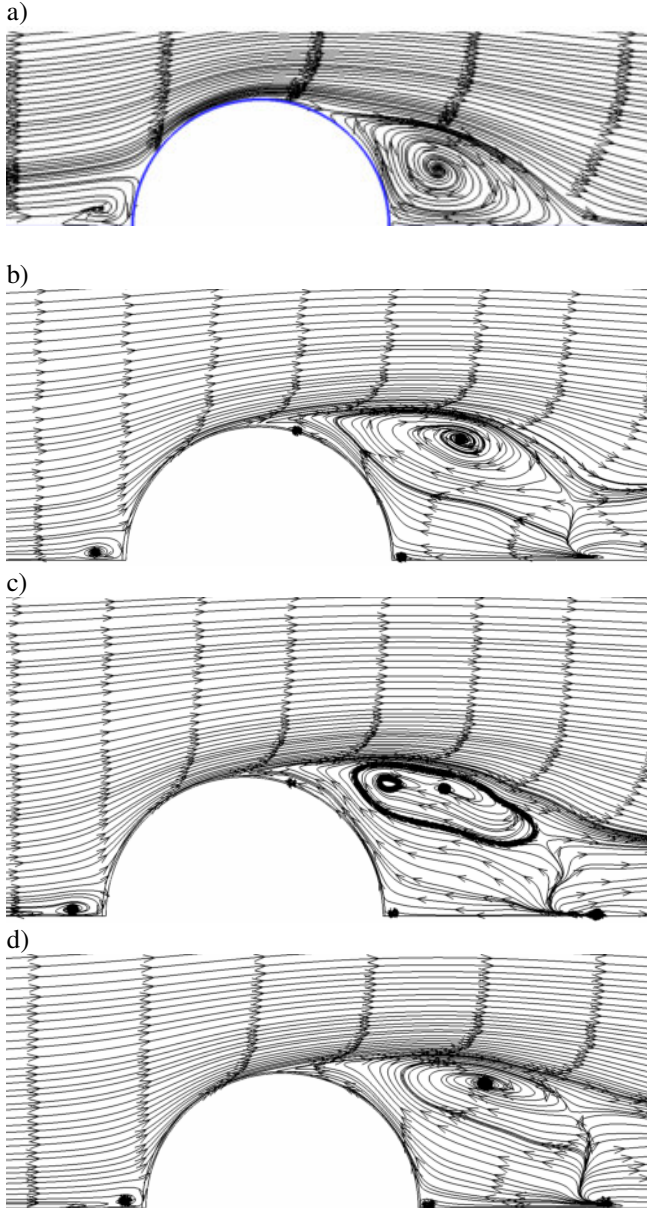
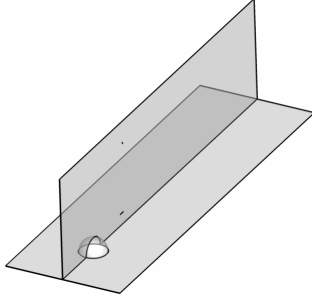


Fig. 5: Typical streamlines at streamwise plane of symmetry, a)RNG, b)LES SM.Dynamic, c)LES KETM, d)LES Wale.

Figure 5 shows the time mean streamlines on plane of symmetry in comparison with the results of RNG $k-\epsilon$ turbulence model. As indicated in this figure a small recirculation zone related to horseshoe vortex is formed in front of hemisphere and a very complex vortical structure is observed behind the hemisphere. The horseshoe vortex forms by means of the accumulation of incoming boundary layer vorticity which is amplified with the adverse pressure gradient due to blockage of hemisphere in the flow domain. The flow reattachment point behind the hemisphere is observable in this figure. The major difference between the prediction of sub-grid scale models and the RNG $k-\epsilon$ model is observed to occur at the recirculation zone behind the hemisphere. The recirculation zone from the sub-grid scale models are extended to upper height behind the hemisphere. A strong vortex behind the hemisphere is distinguished for the various sub-grid scale models with the center located at the height approximately equal to hemisphere height, but the RNG $k-\epsilon$ model predicts the center of this vortex at the middle height of hemisphere. The LES simulation with different sub-grid scale models captures a distinct secondary circulation region at the hemisphere-wall junction behind the hemisphere which is not seen in the prediction of RNG $k-\epsilon$ turbulence model.

Figure 6 depicts the time mean streamlines at plane $Y/H=0.17$ obtained from LES simulation in comparison with the RNG $k-\epsilon$ model. In this figure the separation from the sides of hemisphere and the extension of flow recirculation zone behind the hemisphere are easily observable. Also, two counter rotating vortices are observed behind the hemisphere due to formation of arc-type vortex at the downstream region of hemisphere.

To have a better insight into the flow field in the wake of hemisphere the streamlines at plane $Y/H=0.5$ are plotted in Figure 7. The streamlines at this plane are similar to the plane $Y/H=0.17$. The difference is observed in the extension of shear layer behind the hemisphere which is greater at upper plane ($Y/H=0.5$) located far from the wall. The spanwise extension of shear layer specifies the location of maximum turbulence intensity which is related to maximum velocity gradient at each section in the flow field.

Figure 8 presents the comparison between experimental and numerical streamwise velocity at $X/D=0.67$ on plane of symmetry. The previous result of RNG $k-\epsilon$ turbulence model and prediction of various sub-grid scale eddy viscosity models obtained from present study are compared with the experimental data. Experimental observations indicate that at this section the reversed flow zone extends to the height approximately equal to hemisphere height and then velocity profile approaches to the free stream velocity. Only sub-grid scale models have good prediction of velocity profile at this section. The RNG $k-\epsilon$ schemes do not show a good prediction and underestimate the velocity in the shear layer. The KETM -

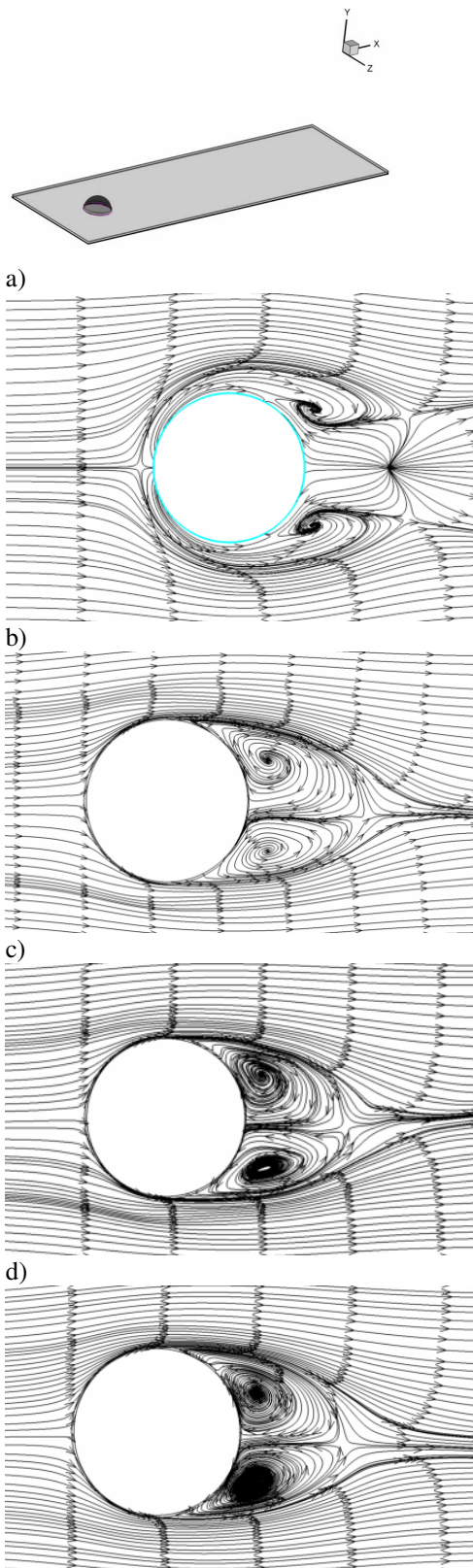


Fig. 6: Typical streamlines at plane $Y/H=0.17$, a) RNG, b) LES SM.Dynamic, c) LES KETM, d) LES Wale.

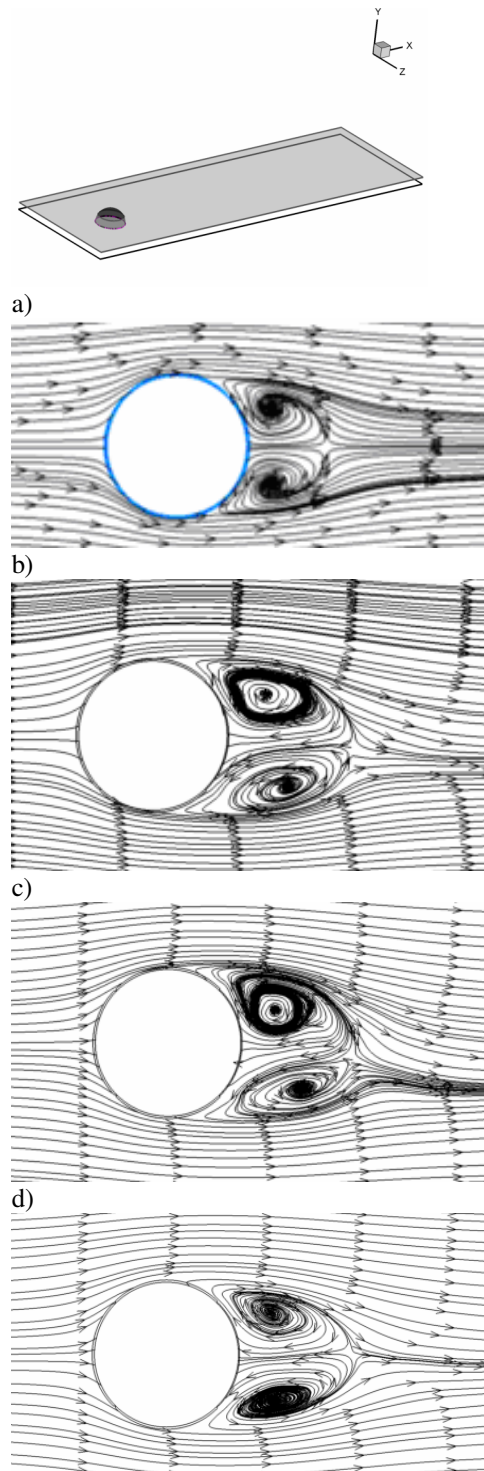


Fig. 7: Typical streamlines at plane $Y/H=0.5$, a) RNG, b) LES SM.Dynamic, c) LES KETM, d) LES Wale.

sub-grid scale eddy viscosity model shows very good agreement with the wind tunnel measurements. The general trends of Smagorinsky dynamic model and WALE model are

good but there are some discrepancies between the results of these models with the experimental data near the wall. The good agreement between the numerical and experimental data is remarkable because of the complexity of flow field around the hemisphere with the separation reattachment process, the existence of curved shear layer and active vortex shedding process. Result of KETM sub-grid scale turbulence model with an additional transport equation is in close agreement with the wind tunnel measurements.

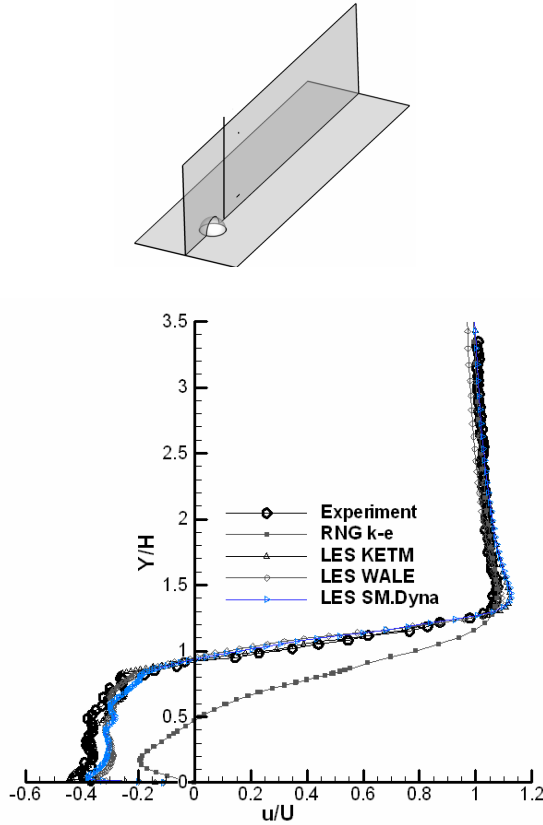


Fig. 8: Comparison between numerical and experimental result at $X/D = 0.67$ on plane of symmetry for 4,200,000 grid cells

Figure 9 depicts the comparison between experimental and numerical streamwise velocity at section $X/D = -0.58$ in front of the hemisphere. As discussed previously, the approaching boundary layer flow upstream of hemisphere is separated from the wall because of the blockage effect of hemisphere and the reverse flow zone forms in front of hemisphere. At this section the prediction of different sub-grid scale models are similar with small discrepancies from the experimental data. More blockage effect of hemisphere is observed in the experimental data compared with that for the sub-grid scale models. Probably, the difference between the numerical and experimental streamwise velocity at this section arises from the fact that the entrance region of tunnel is neglected in the numerical simulation. The development of boundary layer at

this section should be considered to have more accurate prediction of flow field in front of the hemisphere.

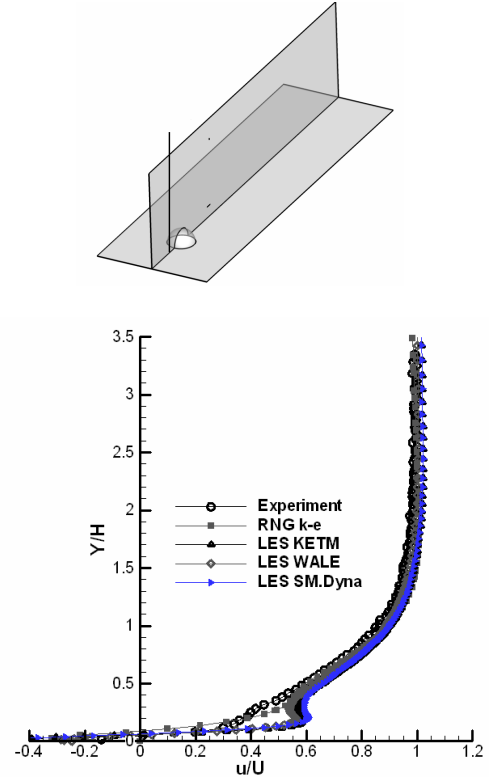


Fig. 9: Comparison between numerical and experimental result at $X/D = -0.58$ on plane of symmetry for 4,200,000 grid cells

Table 1 provides the experimental and numerical results for the mean reattachment length (non-dimensional) behind the hemisphere at streamwise plane of symmetry. The origin of reference coordinate system and the reattachment length are shown at Figure 10. Results show that the prediction of sub-grid scale models for the reattachment length is in good agreement with the wind tunnel measurement.

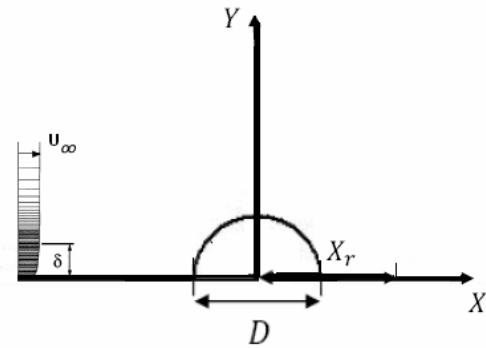


Fig. 10: Reference coordinates and the reattachment length

Table 1: Non-dimensional reattachment length at plane of symmetry

Method	X_r/D
LES (SM. Dynamic)	1.45
LES (KETM)	1.3
LES (Wale)	1.4
RNG k- ϵ [7]	1.4
Exp. [7]	1.25

CONCLUSIONS

Large eddy simulation was employed to simulate the turbulent air flow field around a surface mounted hemisphere. Flow Reynolds number is 30000 based on the free stream velocity and hemisphere diameter. Results are presented for different sub-grid scale models and compared with previous RANS simulation and wind tunnel measurements. Results show that LES simulation especially KETM model with proper grid resolution is able to capture the dynamic behavior of complex flow field formed around the hemisphere. Very good improvement in the prediction of streamwise velocity is distinguished with the high resolution grid in comparison with the low resolution grid. Also, result of present study illustrates that the prediction of LES models is better than RNG k- ϵ in the separated flow behind the obstacle. Therefore, LES is preferable than the classic RANS models for such highly complex turbulent flow field around the curved bluff bodies.

ACKNOWLEDGMENTS

The computations of this study are performed at the high performance computer center in the school of Mechanical Engineering of Shiraz University.

REFERENCES

- [1] Maher, F.J., 1965, "Wind loads on basic dome shapes", *J. Structural Division*, **91**, pp. 219-228.
- [2] Savory, E., Toy, N., 1986, "Hemisphere and hemisphere-cylinders in turbulent boundary layers", *J. Wind. Eng. Ind. Aero.* **23**, pp. 345-364.
- [3] Savory, E., Toy, N., 1988, "The separated shear layers associated with hemispherical bodies in turbulent boundary layers", *J. Wind. Eng. Ind. Aero.* **28**, pp. 291-300.
- [4] Yaghoubi, M.A., 1991, "Air flow patterns around domed roof buildings", *Renewable Energy*, **1**, pp. 345-350.
- [5] Tamura, T., Kuwahara, K., Suzuki, M., 1990, "Numerical study of wind pressures on a domed roof and near wake flows", *J. Wind. Eng. Ind. Aero.*, **36**, pp. 1001-1010.

- [6] Meroney, R.N., Letchford, C.W., Sarkar, P.P., 2002, "Comparison of numerical and wind tunnel simulation of wind loads on smooth, rough and dual domes immersed in a boundary layer", *J. Wind. Structure*, **5**, pp. 219-228.
- [7] Tavakol, M.M., Yaghoubi, M., Masoudi Motlagh, M., 2010, "Air flow aerodynamic on a wall mounted hemisphere for various turbulent boundary layers", *Exp. Thermal and Fluid Sci.*, **34**, pp. 538-553.
- [8] Cheng, C.M., Fu, C.L., 2010, "Characteristic of wind loads on a hemispherical dome in smooth flow and turbulent boundary layer flow", *J. Wind. Eng. Ind. Aero.*, In press.
- [9] Bagget, J.S., Jimenez, J., Kravchenko, A.G., 1997, "Resolution requirements in large eddy simulation of shear flows", *Annual Research Briefs*. Center for Turbulence Research, Stanford university, Stanford, USA.
- [10] Leonard, "The ULTIMATE conservative difference scheme applied to unsteady one-dimensional advection", *Comput. Meth. Appl. Mech. Eng*, **88**, pp 17-74.